Lab on a Chip

Accepted Manuscript

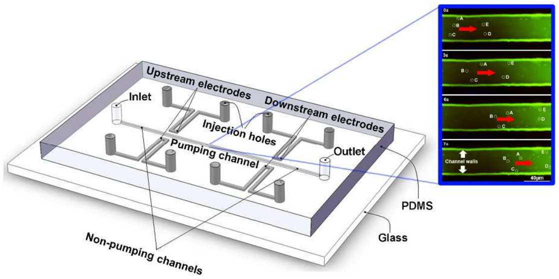

Pumping is as simple as drawing in this handy liquid-metal based electroosmotic flow pump.

Journal Name RSCPublishing

ARTICLE

A handy liquid-metal based electroosmotic flow pump

Cite this: DOI: 10.1039/x0xx00000x

Received 00th January 2013, Accepted 00th January 2013

DOI: 10.1039/x0xx00000x

www.rsc.org/

Meng Gao and Lin Gui*

A room temperature liquid-metal based electroosmotic flow (EOF) pump has been proposed in this work. This low-cost EOF pump is convenient for both fabrication and integration. It utilizes polydimethylsiloxane (PDMS) microchannels filled with the liquid-metal as non-contact pump electrodes. The electrode channels are fabricated symmetrically to both sides of pumping channel, having no contact with the pumping channel. To test the pumping performance of the EOF pump, the mean flow velocities of the fluid (DI water) in the EOF pumps were experimentally measured by tracing the fluorescent microparticles in the flow. To provide guidance for designing low voltage EOF pump, parametric studies on dimensions of electrode and pumping channels were performed in this work. According to the experimental results, the pumping speed can reach 5.93 μm/s at driving voltage of only 1.6 V, when the gap between the electrode and the pumping channel is 20 μm. Injecting room temperature liquid metal into microchannels can provide a simple, rapid, low-cost but accurately self-aligned way to fabricate micro electrodes for EOF pumps, which is a promising method to achieve the miniaturization and integration of the EOF pump in microfluidic systems. The non-contact liquid electrodes have no influence on the fluid in the pumping channel when pumping, reducing Joule heat generation and preventing gas bubble formation at the surface of electrode. The pump has great potential to drive a wide range of fluids, such as drug reagents, cell suspensions and biological macromolecule solutions.

Introduction

Micropumps are key components of microfluidic systems.[1–2] They have so far been used in various areas, including biological/chemical analysis,[3-5] liquid drug delivery[6] and microelectronic equipment cooling[7]. With the development of microfluidic technologies, there is an increasing demand for fluid pumping techniques with a wide range of flow rates, controllable delivery, compact design, simple fabrication and efficient operation.[8–9]

Electroosmotic flow (EOF) pumps have attracted a great deal of attention because of their ability to generate high pumping pressure with continuous pulse-free flow.[10–11] These pumps can also offer precision delivery of small volumetric fluids.[12–13] Notably, by changing the strengths and directions of the applied electric fields through the pumping channels, the fluid flow magnitudes and directions of the EOFs can be controlled conveniently. The EOF pumps have no moving parts, which can be fabricated and integrated easily into lab-on-a-chip systems.[14–15] Generally, the EOF pumps can be divided into two categories: (i) porous media based EOF pumps[16–21] and (ii) direct EOF pumps[22–26]. The former involves a large number of porous dielectric materials, porous membranes or microparticles packed in the pumping microchannels, forming electroosmotic sub-microchannels or nanochannels. By applying operation voltage on the porous media, the electroosmotic flows in the porous media can provide very high pumping pressures and sometimes high-rate flows. However, the fabrication techniques for the porous dielectric media microstructures are cost-expensive, and non-compatible with the pumping microchannel fabrication process, leading to an obvious limit for the integration of micropumps into lab-on-a-chip systems. Actually, because the porous media "blocks" the main pumping channel, these porous media based EOF micropumps cannot delivery large particles such as cells or biological macromolecules in the pumping channel. On the contrary, the direct EOF pumps apply voltage direct on the pumping channel and have nothing blocking the pumping channel. Larger particles can be easily delivered in this type of EOF pump. Because the structure of the direct EOF pump is much simpler than the porous media based EOF pump, the direct EOF pump can be easily miniaturized and integrated into a microfluidic chip.

Electrodes are essential for EOF pumps to provide an efficient pumping performance. Electrode material and fabrication technique play important roles in cost control and integration of electrodes in EOF pumps.[27,28] Traditionally, electrodes for the EOF pumps are made of solid inert-metal, such as platinum (Pt) or gold (Au). Solid electrodes can be divided into three categories, including mesh micro electrodes[16], membranous micro electrodes[22] and wire electrodes[26]. The mesh micro electrodes are placed on both ends of the porous channels, which can provide a roughly uniform electric field. The membranous micro electrodes are often sputtered or deposited under the pumping channel. These two types of electrodes can be well miniaturized and integrated into the pumping system. However, they have to be aligned with the pumping microchannel very accurately in the fabrication process. Thus the fabrication technique for these electrodes requires an extra precision and high-cost micro fabrication system. The wire electrodes are directly inserted into the inlet/outlet reservoirs of the pumping channel, which are the simplest type of electrodes for EOF pumps but not suitable for integration. These electrodes are directly exposed to the pumping fluid in the pump, thus the fluid electrolysis can easily take place near the non-inert-material electrodes generating gas bubbles and electrode corrosion. Sometimes, these exposed electrodes will generate other serious problems, such as undesirable electrolytic products, short circuit of high voltage supply equipment and Joule heat formation in the pumping fluid.[14,17,29] As a result, the electroosmosis mobility and flow rate will decrease greatly.[30] Recently, bubbleless electrodes have been proposed to eliminate bubble formation in the pumping fluid, such as gel-type salt bridge electrodes[31] and vinylzed fused silica capillary electrodes[32]. However, these bubbleless electrodes have also contact with the pumping fluid directly, leading to the problem of Joule heat formation in the pumping fluid while the pump works with high voltages. Meanwhile, the fabrication of these bubbleless electrodes also requires a relatively complex fabrication process and high cost.

Non-contact conductive liquid microfluidic electrodes are ideal for EOF pumps to prevent above limitations. The non-contact microelectrodes were fabricated by injecting conductive liquid into microchannels located at both sides of the pumping channel. Compared with the solid electrodes, conductive liquid material is more suitable for non-contact microfluidic electrodes due to its simple, low-cost injection technique and easy alignment. Among conductive liquid, wettable liquid metal[35,36] has been demonstrated to be a promising material for microfluidic electrodes due to its good electrical conductivity together with non-volatility in gas permeable microchannels, such as PDMS microchannels. Recently, room temperature liquid-metal (gallium or gallium-base alloy) has been widely used to form microelectrodes in microchannels using simple injection technique due to its favourable properties, in terms of low melting point and handy deformability.[33–35] Applications of this liquid metal in micro-chips have been developed, such as microelectrodes,[34,35] microstructures,[33,36] and microfluidic electronics[37–42]. Injecting liquid metal into microchannels provides a very simple and low-cost technique to fabricate liquid electrodes. These electrodes are very convenient for chip design and can be fabricated in any shape, integrated into a microfluidic chip at any location and, meanwhile, with high accuracy of alignment. The microchannels for liquid metal are fabricated together with the pumping channel just in the same step using the same fabrication technique. More important, the solid gallium oxide layer easily generated on the surface of the liquid metal can help to stabilize the microstructure of these liquid electrodes in PDMS microchannels.

In this work, a handy EOF pump using liquid metal microelectrodes was proposed. Then the EOF pump was fabricated and tested. To achieve a low voltage EOF pump, parametric studies were performed in detail in this research. Fluorescent particles were used to trace the pumping flow during the experiments.

Liquid-metal based EOF pump

Figure 1 shows the schematic of the liquid-metal based EOF micro pump embedded in a PDMS/Glass microfluidic chip. The EOF pump utilizes microchannels filled with liquid metal to form non-contact electrodes of the pump. The chip is 3 cm long, 1.5 cm wide, and 3 mm thick (1 mm thick glass slide and 2 mm thick PDMS slab). As shown in Fig. 1, two pairs of electrode channels filled with liquid metal are fabricated symmetrically to both sides of the pumping channel in the same horizontal plane of the microfluidic chip. These two pairs of electrode channels are also designed parallel to each other and vertical to the pumping channel. The electrodes are placed very close to but not contact with the pumping channel. For the convenience of injecting liquid metal, all the electrode channels are designed in ohm shape, with both injection inlet and outlet 5 mm away from the pumping channel. An advantage of this micro electrode is that, compared with direct-contact inert-metal electrodes, the liquid-metal electrodes have no contact with the microfluid and thus, have no influence on the pumping fluid during pumping.

Although the chip material, PDMS, has very high electrical resistivity, because the gap between the electrodes and the pumping channel is very small (≤40 μm in this work) compared with the pumping channel length, electric field can be still induced along the pumping channel while high voltage is applied. Using the ohm-shape electrodes, the electric field generated between the electrodes is uniform and parallel to the pumping channel (see Fig. 2). Thus, the induced electric field strength along the pumping channel wall can drive the electrical double layer (EDL) at the solid-liquid interface of the pumping channel, generating electroosmotic flow in the pumping channel. For better understanding how the EOF pump works, numerical simulation of the electric field distribution inside the pumping channel was performed. Limited to the length of the paper, the simulation was included in the Electronic Supplementary Information (ESI).

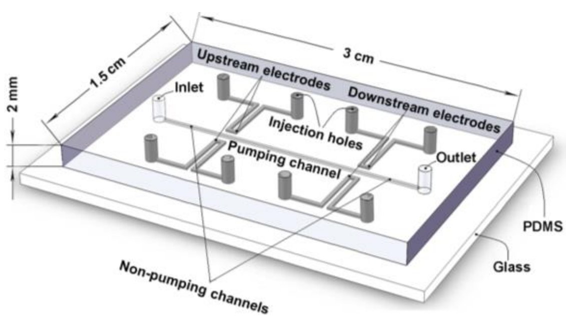

Fig. 1 Schematic of PDMS/Glass microfluidic chip with liquid-metal micro ohm-shape electrodes embedded for EOF pump.

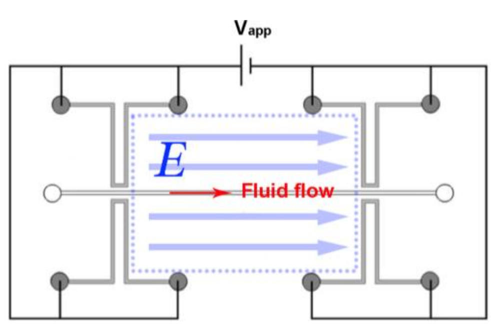

Fig. 2 Schematic of working principle of liquid-metal based EOF pump.

Experimental details

Fabrication

The fabrication of PDMS microfluidic chips for EOF pumps was performed using standard soft-lithography technique. SU-8 2050 and 2005 (MicroChem Corp.) were used to fabricate 50 μm and 5 μm high microchannels, respectively. Sylgard 184 silicone elastomer[43] (mixture of base and curing agent at a 10:1 ratio per weight, Dow Corning Corp.) was used to make the PDMS microfluidic chips. The irreversible enclosed microchannels were fabricated by bonding the patterned PDMS slab with a glass slide (76 mm×25 mm×1 mm) using the air plasma treatment (plasma cleaner, YZD08-2C, Tangshan Yanzhao Technology).

Figure 3 shows the optical photograph of the PDMS microfluidic chip with liquid metal electrodes embedded for the EOF pump. The liquid-metal alloy $GaIn_{20.5}Sn_{13.5}$ (Ga 66%, In 20.5%, Sn 13.5%; melting point, 10.6 ℃)[44] was used to form the pump electrodes by injecting it into the electrode channels.[35,37] Fine copper wires (diameter 150 μm) were then inserted into the injection holes and kept good contact with liquid metal inside. To fasten the connection, the conjunction of copper wire and liquid metal was sealed with a package adhesive sealant (705 RTV Transparent Silicone Rubber).

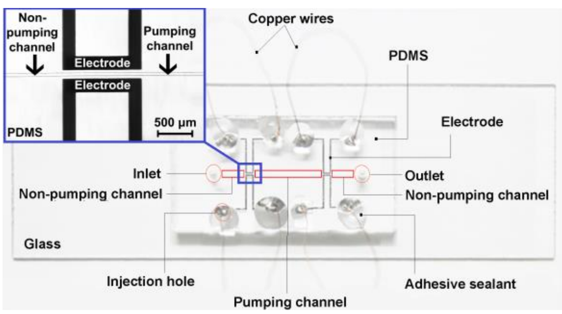

Fig. 3 Optical photograph of PDMS microfluidic chip with liquid metal electrodes embedded for EOF pump. The subfigure shows the liquid metal electrodes of the EOF pump. The PDMS gap is 40 μm. The pumping channel is 40 μm wide, 1 cm long. The non-pumping channel is 2 mm long and the electrode channel is 200 μm wide.

Measurement of flow velocity

For all experiments, deionized (DI) water was used as the pumping fluid. The pumping channels were immediately filled with DI water after chip bonding.[45] A high voltage sequencer (HVS448 6000D, LabSmith, Inc.) was used to offer high voltages for the EOF pumps. Low voltages (less than 10 V) were offered by ordinary dry batteries (1.6 V and 4 V). 0.5 μm fluorescent polystyrene particles (Ex 542 nm, Em 612 nm, 1% solids, Duke Scientific Corporation) were diluted 1000 times, and then used as tracing particles for the flow speed measurement. After loading fluid into the microchannels, the inlet and outlet reservoirs were covered with two droplets. Because of the difference of the droplets, static pressure difference was first induced inside the microchannel. After self-balance of 30 minutes, the fluid inside the microchannel stopped flowing and the microfluidic chip was ready for pumping test. A fluorescence microscope (Axio Observer Z1, Carl Zeiss) was used to monitor the pumping process. Five particles with different distance to the channel wall were randomly chosen and traced to calculate the mean flow velocity of the electroosmotic flow.

Parametric studies

To provide guidance for designing EOF pump, parametric studies were performed in this research. Five parameters were considered, including the PDMS gap (30 μm and 40 μm), the pumping channel length (100 μm and 1 cm) and width (30 μm and 40 μm), the non-pumping channel length (2 mm and 7 mm) and the channel height (5 μm and 50 μm), as shown in Fig. 4. The electrode channels are 200 μm wide. The injection inlets and outlets of electrode channels are 5 mm away from the pumping channel. The distance between the injection inlet and outlet along the pumping channel is 1.1 cm. The head of the electrode is 1 mm long along the pumping channel.

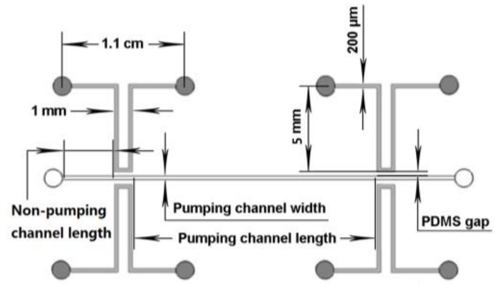

Fig. 4 Schematic of dimensions of liquid-metal electrodes and pumping channel in PDMS/Glass microfluidic chip for EOF pump.

Results and discussion

What should be pointed out before the experimental result is that, although the PDMS material has very high electrical resistivity, when the PDMS gap between the electrodes and the pumping channel is small enough (⩽40 μm, much smaller than pumping channel length), it can work as a normal resistor, letting charges getting through it. The charges continuously come out from one electrode and go back to the other, with no charges accumulated in the microchannel. Thus, the pump can keep pumping for a long time. During all the experiments performed below, the pumps keep working for at least two hours without any slowing down. In another word, the PDMS gap may act like an ion exchange membrane that allows charges getting through it but stops the water molecules. The mechanism is similar to the gel-type salt bridge electrodes[31].

Sequential images of fluorescent particle movements in EOF

Figure 5 shows the sequential images of fluorescent particle movements in the electroosmotic flow at different relative times. The images were taken from one continuous electroosmotic flow. In these images, the pumping channel is 1 cm long, 40 μm wide. The non-pumping part is 2 mm long. All channels are 50 μm high. The PDMS gap is 40 μm. The applied voltage is 50V. Capital letters (A, B, C, D and E) and circle marks represent five particles with different distances to the channel wall. As shown in Fig. 5, the mean velocity of electroosmotic flow in the pumping channel is determined to be 12.34 μm/s by measuring the movements of five fluorescent particles within 7 seconds.

One interesting thing is that, if compare 0s with 3s, one can observe that particle A and C move much faster than particle B and D (Particle E moves from the centre to the side, not parallel to the flow direction). That is because particle A and C are very close to the pumping channel wall, and the electroosmotic flow is driven by the moving electrical double layer near the pumping channel wall.

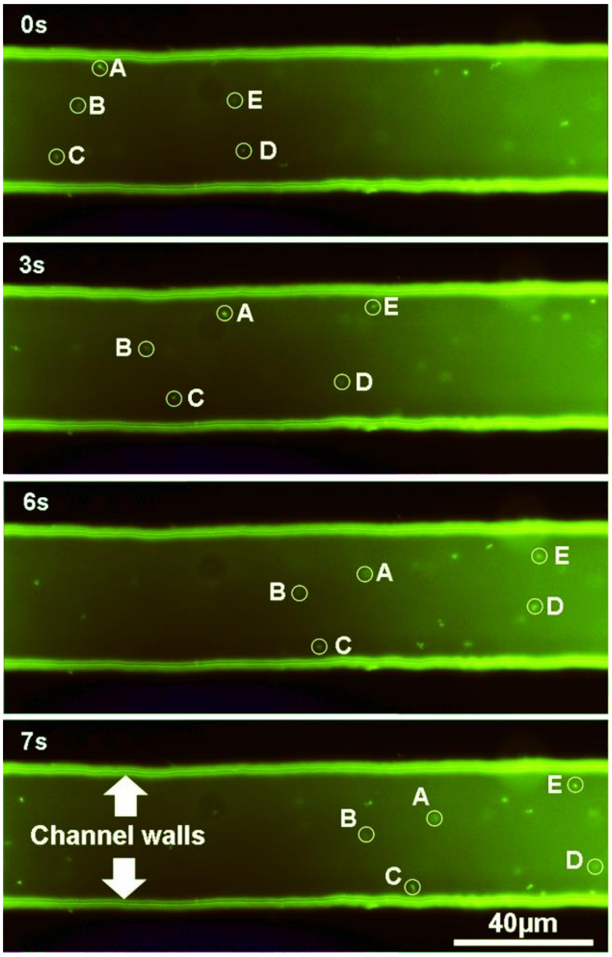

Fig. 5 Sequential images of fluorescent particles in electroosmotic flow in the pumping channel at different relative times (40 μm PDMS gap, 40 μm wide, 1 cm long pumping channel, 2 mm long non-pumping channel, 50 μm high channel, 50 V applied voltage). A, B, C, D and E and circle marks represent five tracing fluorescent particles.

Experimental results of parametric studies

Figure 6 (a) shows the mean electroosmotic flow velocity in the pumping channel as a function of voltage applied with different PDMS gap and pumping channel width (30 μm design and 40 μm design). In all the experiments, the pumping channel is 1 cm long. The non-pumping part is 2 mm long. All channels are 50 μm high. As shown in Fig. 6 (a), the mean electroosmotic flow velocity of the pump almost linearly increases with the increment of the applied voltage. The pump with 30 μm PDMS gap and 30 μm wide pumping channel (30 μm pump) can drive the DI water flow to 10.67 μm/s at 25 V. Compared with 40 μm design, the flow velocity driven by 30 μm pump increases 40%~50%. Thus the PDMS gap or the pumping channel width is key to the mean electroosmotic flow velocity of the pump. Smaller PDMS gap and narrower pumping channel can help improve the high electroosmotic flow velocity of the pump. In other words, the pump with smaller PDMS gap and narrower pumping channel can successfully drive the flow at a lower voltage. In this research, PDMS gap is recommended to be around 30~40 μm. Smaller gap will increase the difficulty of fabrication, and larger gap will decrease the efficiency of the EOF pump dramatically. Extreme test shows that the liquid metal electrodes of 30 μm design will be damaged, when the voltage reaches 1800V (1 cm long pumping channel). Before the breaking down, the pump reaches its highest possible pumping velocity of 760 μm/s.

Figure 6 (b) shows the mean fluid flow velocity in the pumping channel as a function of voltage applied with different pumping channel length. Two types of pumping channel length are considered: 100 μm and 1cm. The pumping channel width and the PDMS gap are 40 μm. The non-pumping part is still 2 mm long. Channel height is 50 μm. As shown in Fig. 6 (b), the pump with 100 μm long pumping channel can drive the DI water flow to 7.08 μm/s at 15 V. However, the pump with 1 cm long pumping channel cannot drive the flow when the voltage is less than 25V. For the 100 μm pump design, although the non-pumping part (2 mm long) is 20 times longer than the pumping part (100 μm), the pumping strength is far strong enough to overcome the flow resistance in the non-pumping part. Smaller pumping channel length will help decrease the voltage requirements. But too small pumping channel length will also shrink the pumping area and decrease the pumping energy. 100 μm is recommended to be the low limit of the pumping length of the 40 μm gap design. Extreme test shows that the liquid metal electrodes will be damaged, when the voltage reaches 450V (100 μm long pumping channel). Before the breaking down, the pump reaches its highest possible pumping velocity of 270 μm/s.

It is well known that the fluid flow in microchannels has high flow resistance due to the large surface-area-to-volume ratio of microchannel. In EOF pumps, the fluid flow resistance mainly comes from the wall friction of the non-pumping channel. Increasing the length of the non-pumping part or decrease the cross section area of the non-pumping channel will significantly increase the fluid flow resistance. Figure 6 (c) shows the mean fluid flow velocity in the pumping channel as a function of voltage with different non-pumping channel length. The pumping channel width and the PDMS gap are 40 μm. The pumping channel is 1 cm long. All channels are 50 μm high. It can be seen clearly from Fig. 6 (c) that the pump with 2 mm long non-pumping channel can drive the flow to 6.06 μm/s in the pumping channel at 25 V. However, the pump with 7 mm long non-pumping channel can only drive the flow to 5.62 μm/s even at 300 V. Thus, to obtain a high fluid flow velocity at a certain applied voltage, the fluid flow resistance in the non-pumping channel should be considered as an important factor. Besides, increasing the non-pumping channel width or height is obviously another effective method to reduce the fluid flow resistance.

In some circumstances, for example in implantable medical devices, high voltage is not feasible for pumping fluid. Thus, low voltage EOF pump is a promising pumping method in medical use. Figure 6 (d) shows the mean electroosmotic flow velocity as a function of voltage at different channel height. The Figure also shows a low voltage EOF pump we designed (less than 10 V). The pumping channel is 20 μm wide and 100 μm long. The non-pumping channel is 2 mm long (20 times longer than the pump length). The PDMS gap is 20 μm. Two types of channel height are considered (5 μm and 50 μm). As shown in Fig. 6 (d), the pump with 50 μm high channel can successfully drive the flow to 5.93 μm/s at only 1.6 V, which means just one dry battery is capable of driving this pump. Due to the high flow resistance in the 5 μm high channel, the 5 μm pump can only drive the flow to 4.21 μm/s at 4 V.

Journal Name RSCPublishing

ARTICLE

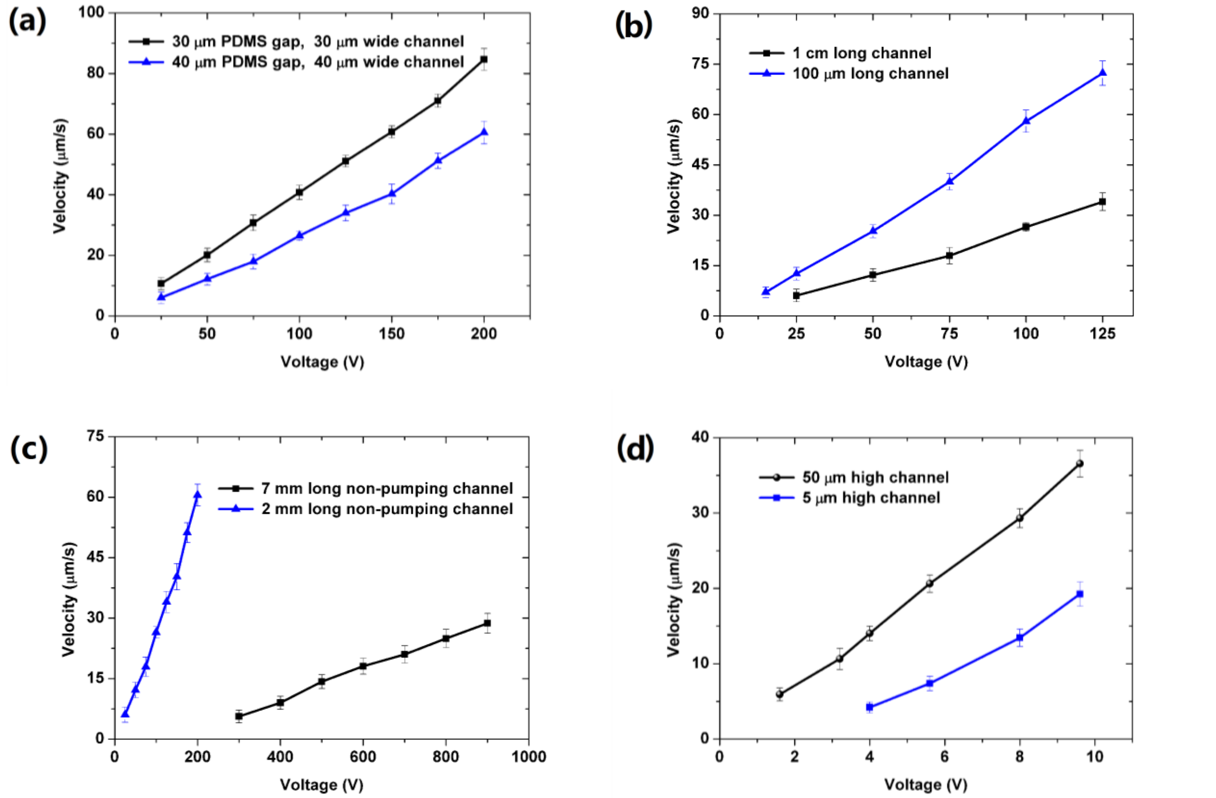

Fig. 6 Experimental results of parametric studies. (a) Flow velocity as a function of voltage with different PDMS gap and pumping channel width (The pumping channel is 1 cm long. The non-pumping channel is 2 mm long. All channels are 50 μm high.); (b) Flow velocity as a function of voltage at different pumping channel length (The pumping channel width and the PDMS gap are 40 μm. The non-pumping channel is 2 mm long. All channels are 50 μm high.); (c) Flow velocity as a function of voltage at different non-pumping channel length (The pumping channel width and the PDMS gap are 40 μm. The pumping channel is 1 cm long. All channels are 50 μm high.); (d) Flow velocity as a function of voltage at different channel height (The pumping channel is 20 μm wide and 100 μm long. The non-pumping channel is 2 mm long. The PDMS gap is 20 μm.).

Conclusions

In this study, the utilization of liquid-metal based micro electrodes in EOF pumps has been proposed and demonstrated. Micro channels are filled with liquid metal, work as micro electrodes of the EOF pump. To achieve low voltage EOF pump, parametric studies were experimentally performed to investigate the pump design. The results show that with 20 μm PDMS gap and 100 μm long pumping channel, the pump can drive the flow to 5.93 μm/s at a low voltage of only 1.6 V. Pumping velocity may be further improved by using even smaller PDMS gap or higher non-pumping channels.

In the near future, for high velocity pumping solution, one can follow the design guideline of 30 μm pump design with 1cm long pumping channel (~1 cm) and higher voltage (but less than 1800 V). For low voltage (less than 5 V) pumping solution, one can follow the pump design shown in Fig. 6 (d) with smaller PDMS gap (~20 μm), shorter pumping length (~100 μm) and higher channel height (~50 μm).

Using liquid-metal-filled microchannels as embedded micro electrodes can provide an efficient approach to the miniaturization and integration of the EOF micro pump in microfluidic systems. The liquid-metal microchannels can be fabricated just in one step together with the pumping channel using the same fabrication technique. Due to the flowability and deformability of liquid metal, the electrodes can be easily achieved in any shape at any location. Another merit for the EOF pumps using non-contact liquid-metal electrodes is that, compared with the pumps using direct-contact solid-metal electrodes, these EOF pumps will effectively reduce Joule heat generation, as well as prevent gas bubble formation, electrode corrosion/polarization, electrolysis and cross contamination between the electrodes and the fluid. In the near future, the EOF pump should be a promising microdevice used to drive cell/macromolecule solutions or drug reagents.

Acknowledgements

This work is financially supported by the National Natural Science Foundation of China (Grant No. 51276189).

Notes and references

Key Laboratory of Cryogenics, Technical Institute of Physics and Chemistry, Chinese Academy of Sciences, Beijing, 100190, P. R. China, Fax/Tel: +86 10 8254 3483; E-mail: lingui@mail.ipc.ac.cn
†Electronic Supplementary Information (ESI) available. See DOI: 10.1039/b000000x/

1 J. Rupp, M. Schmidt, S. M€unch, M. Cavalar, Ulf Steller, J. Steigert, M. Stumber, C. Dorrer, P. Rothacher, R. Zengerled and M. Daub, *Lab Chip*, 2012, **12**, 1384–1388.
2 A. B. Wang and M. C. Hsieh, *Lab Chip*, 2012, 12, 3024–3027.
3 C. Zhang, D. Xing and Y. Li, *Biotechnol. Adv*., 2007, **25**, 483–514.
4 J. Li, C. Liu, Z. Xu, K. Zhang, X. Ke, C. Li and L. Wang, *Lab Chip*, 2011, **11**, 2785–2789.
5 R. Shabania and H. Jin Cho, *Lab Chip*, 2011, **11**, 3401–3403.
6 A. Nisar, N. Afzulpurkar, B. Mahaisavariya and A. Tuantranont, *Sens. Actuators B*, 2008, **130**, 917–942.
7 Y. Berrouche, Y. Avenas, C. Schaeffer, H. C. Chang and P. Wang, *IEEE Trans. Indus. Appl.*, 2009, **45**, 2073–2079.
8 A. Ezkerra, L. Jose Fernandez, K. Mayora and J. M. Ruano-Lopez, *Lab Chip*, 2011, **11**, 3320–3325.
9 G. H. Kwon, G. S. Jeong, J. Y. Park, J. H. Moon and S. H. Lee, *Lab Chip*, 2011, **11**, 2910–2915.
10 L. J. Jin, J. Ferrance, J. C. Sanders and J. P. Landers, *Lab Chip*, 2003, **3**, 11–18.
11 L. J. Nelstrop, P. A. Greenwood and G. M. Greenway, *Lab Chip*, 2001, **1**, 138–142.
12 S. Debesset, C. J. Hayden, C. Dalton, J. C. T. Eijkel and A. Manz, *Lab Chip*, 2004, **4**, 396–400.
13 C. K. Harnett, J. Templeton, K. A. Dunphy-Guzman, Y. M. Senousy and M. P. Kanouff, *Lab Chip*, 2008, **8**, 565–572.
14 X. Y Wang, C. Cheng, S. L. Wang, S. R. Liu, *Microfluid. Nanofluid.*, 2009, **6**, 145–162.
15 X. Y. Wang, S. L. Wang, B. Gendhar, C. Cheng, C. K. Byun, G. B. Li, M. P. Zhao, S. R. Liu, *Trends Anal. Chem.*, 2009, **28**, 64–74.
16 C. M. Wang, L. Wang, X. R. Zhu, Y. G. Wang and J. M. Xue, *Lab Chip*, 2012,**12**, 1710–1716.
17 Y. Ai, S. E. Yalcin, D. F. Gu, O. Baysal, H. Baumgart, S. Z. Qian, A. Beskok, *J. Colloid Interface Sci.*, 2010, **350**, 465–470.
18 Y. F. Chen, M. C. Li, Y. H. Hu, W. J. Chang, C. C. Wang, *Microfluid. Nanofluid.*, 2008, **5**, 235–244.
19 A. Brask, D. Snakenborg, J. P. Kutter and H. Bruus, *Lab Chip*, 2006, **6**, 280–288.
20 Z. L. Chen, P. Wang and H. C. Chang, *Anal. Bioanal. Chem.*, 2005, **382**, 817–824.
21 A. Brask, J. P. Kutter and H. Bruus, *Lab Chip*, 2005, **5**, 730–738.
22 A. Jahanshahi, F. Axisa, J. Vanfleteren, *Microfluid. Nanofluid.*, 2012, **12**, 771–777.
23 T. Glawdel and C. L. Ren, *Mechan. Res. Commun.*, 2009, **36**, 75–81.
24 P. Wang, Z. L. Chen and H. C. Chang, *Sens. Actuators B*, 2006, **113**, 500–509.
25 I. M. Lazar and B. L. Karger, *Anal. Chem.*, 2002, **74**, 6259–6268.
26 J. M. Edwards IV, M. N. Hamblin, H. V. Fuentes, B. A. Peeni, M. L. Lee, A. T. Woolley and A. R. Hawkins, *Biomicrofluidics*, 2007, **1**, 014101–11.
27 F. Q. Nie, M. Macka and B. Paull, *Lab Chip*, 2007, **7**, 1597–1599.
28 T. Glawdel, C. Elbuken, L. E. J. Lee and C. L. Ren, *Lab Chip*, 2009, **9**, 3243–3250.
29 S. R. Liu, Q. S Pu and J. J. Lu, *J. Chromatogr. A*, 2003, **1013**, 57–64.
30 D. G. Strickland, M. E. Suss, T. A. Zangle and J. G. Santiago, *Sens. Actuators B*, 2010, **143**, 795–798.
31 Y. Takamura, H. Onoda, H. Inokuchi, S. Adachi, A. Oki and Y. Horiike, *Electrophoresis*, 2003, **24**, 185–192.
32 C. Y. Gu, Z. J. Jia, Z. F. Zhu, C. Y. He, W. Wang, A. Morgan, J. J. Lu, and S. R. Liu, *Anal. Chem*., 2012, **84**, 9609−9614.
33 A. C. Siegel, D. A. Bruzewicz, D. B. Weibel and G. M. Whitesides, *Adv. Mater.*, 2007, **19**, 727–733.
34 J. H. So and M. D. Dickey, *Lab Chip*, 2011, **11**, 905–911.
35 J. H. So, H. J. Koo, M. D. Dickey and O. D. Velev, *Adv. Funct. Mater.*, 2012, **22**, 625–631.
36 M. D. Dickey, R. C. Chiechi, R. J. Larsen, E. A. Weiss, D. A. Weitz and G. M. Whitesides, *Adv. Funct. Mater.*, 2008, **18**, 1097–1104.
37 J. H. So, J. Thelen, A. Qusba, G. J. Hayes, G. Lazzi and M. D. Dickey, *Adv. Funct. Mater.*, 2009, **19**, 3632–3637.
38 R. C. Chiechi, E. A. Weiss, M. D. Dickey and G. M. Whitesides, *Angew. Chem. Int. Ed*., 2008, **47**, 142–144.
39 E. Palleau, S. Reece, S. C. Desai, M. E. Smith and M. D. Dickey, *Adv. Mater.*, 2013, 25, 1589–1592.
40 S. H. Jeong, A. Hagman, K. Hjort, M. Jobs, J. Sundqvist and Z. G. Wu, *Lab Chip*, 2012, **12**, 4657–4664.
41 S. Cheng and Z. G. Wu, *Lab Chip*, 2012, **12**, 2782–2791.
42 S. Cheng and Z. G. Wu, *Lab Chip*, 2010, **10**, 3227–3234.
43 J. Mark, Polymer Data Handbook, Oxford Univ. Press, 1999, p425.
44 M. Gao, L. Gui and J. Liu, *J. Heat Transfer*, 2013, **135**, 091402–8.
45 X. Q. Ren, M. Bachman, C. Sims, G. P. Lia and N. Allbritton, *J. Chromatogr. B*, 2001, **762**, 117–125.

